Diagnosis of physical and biological control over phytoplankton in the Gulf of Maine-Georges Bank region using an adjoint data assimilation approach

J. Ocean Univ. China (Oceanic and Coastal Sea Research)
DOI 10.1007/s11802-014-1995-9
ISSN 1672-5182, 2014 13 (3): 356-368
http://www.ouc.edu.cn/xbywb/
E-mail:xbywb@ouc.edu.cn

Diagnosis of Physical and Biological Control over Phytoplankton in the Gulf of Maine-Georges Bank Region Using an Adjoint Data Assimilation Approach

WANG Caixia[1), *], and Paola Malanotte-Rizzoli[2)]

1) *Physical Oceanography Laboratory*, *Ocean University of China*, *Qingdao* 266100, *P. R. China*
2) *Department of Earth*, *Atmospheric and Planetary Sciences*, *Massachusetts Institute of Technology*, *Cambridge*, *MA* 02139, *USA*

(Received March 29, 2012; revised June 11, 2012; accepted July 30, 2013)

Abstract The linkage between physical and biological processes, particularly the effect of the circulation field on the distribution of phytoplankton, is studied by applying a two-dimensional model and an adjoint data assimilation approach to the Gulf of Maine-Georges Bank region. The model results, comparing well with observation data, reveal seasonal and geographic variations of phytoplankton concentration and verify that the seasonal cycles of phytoplankton are controlled by both biological sources and advection processes which are functions of space and time and counterbalance each other. Although advective flux divergences have greater magnitudes on Georges Bank than in the coastal region of the western Gulf of Maine, advection control over phytoplankton concentration is more significant in the coastal region of the western Gulf of Maine. The model results also suggest that the two separated populations in the coastal regions of the western Gulf of Maine and on Georges Bank are self-sustaining.

Key words physical circulation; biological source; adjoint data assimilation

1 Introduction

Photosynthesis in the oceans, the conversion of solar energy to chemical energy, is a fundamental step by which inorganic carbon is fixed by algae and converted into primary production. Significant rates of primary production can occur only in the well-lit euphotic zone. Hence, the animals which feed on the primary production can survive mostly within the mixed layer where there are high levels of food for them. Physical processes play an important role in marine ecosystem dynamics (Collins *et al.*, 2009; Denman and Pena, 2002; Wang and Malanotte-Rizzoli, 1999; Mann and Lazier, 1991) and can modify or limit biological production through the nutrients supply and mean irradiance field (*e.g.*, McClain *et al.*, 1990; Mitchell *et al.*, 1991).

The depth of the mixed layer, the intensity of the solar radiation penetrating into water column, and the vertical distribution of the dissolved nutrients are some of the major factors regulating the biosystem of the sea. The seasonal variation in the atmosphere-ocean heat flux imparts a seasonal cycle to the depth of the mixed layer (Menzel and Ryther, 1960). The variation of wind stress also affects the depth of the mixed layer, and the horizontal flow field does affect the biological system (Campbell, 1986; Flierl and Davis, 1993; Franks and Chen, 1996; McGillicuddy *et al.*, 1998).

Georges Bank constitutes one of the most productive shelf ecosystems in the world (O'Reilly *et al.*, 1987; Cohen and Grosslein, 1987), having an annual area-weighted production two-to-three times that of the world's average for continental shelves. Inter-disciplinary field programs examining the physics and biology of the region have shown the high production rates being closely linked to the unusual circulation dynamics on the Bank (*e.g.*, Riley, 1941; Cohen *et al.*, 1982; Home *et al.*, 1989). A two-dimensional (x, z) coupled physical-biological model of the plankton on Georges Bank during summer was developed by Franks and Chen (1996). In their study, the physically forced vertically integrated fluxes of phytoplankton, zooplankton, and nutrients on and off the Bank were quantified, with the biological variables behaving as conservative, passive tracers. Their study showed that the largest changes occurred within the fronts, where biochemicals including nutrients, phytoplankton, and zooplankton were transported from deep waters toward shallow waters of the Bank. The phytoplankton field became vertically homogeneous over the Bank, with slightly decreasing concentrations from south to north. A patch of high phytoplankton biomass formed in the northern tidal front.

* Corresponding author. E-mail: cxwang@ouc.edu.cn

The geomorphological, physical, chemical, and biological characteristics of the Gulf of Maine are reasonably consistent with the concept of an estuary (Campbell, 1986). One of the prominent characteristics of estuaries is that the import and export of materials and organisms play important roles in controlling biological production within the system (Margalef, 1967). Riley (1967) studied the effects of shoreward nutrient transport on the productivity of coastal waters off southern New England. He concluded that nutrient transport was an important factor for the distribution of biological productivity across the continental shelf.

Intensvie modeling activities have been carried out in the Gulf of Maine-Georges Bank region. Lynch *et al.* (1996) employed a finite element approach to facilitate realistic representation of the complex geometry in this area. The model is three dimensional, hydrostatic, and fully nonlinear, and a level 2.5 turbulence closure scheme (Mellor and Yamada, 1982) is incorporated in the model to study the vertical mixing of momentum, heat and mass. The calculated climatological circulation compares well with available observations (Naimie, 1996; Lynch *et al.*, 1997). The solutions are separated into six bi-monthly periods, which form the inputs to the two-dimensional ADR (advection-diffusion-reaction) equation on the same grid. Boundary conditions used to solve the ADR equation are 1) no flux through solid boundaries, 2) concentration at the inflow is specified, and 3) concentration at the outflow is computed with no diffusion assumption.

Data assimilation techniques have been successfully applied in meteorology and are routinely used in operational weather forecast models. More recently, these techniques have been used in ocean circulation models. Reviews of data assimilation methods as applied in meteorology and oceanography are found in Bengtsson *et al.* (1981), Lorenc (1986), Haidvogel and Robinson (1989), and Ghil and Malanotte-Rizzoli (1991). In the field of biological oceanography where satellite systems and other continuously-recording instruments provide large quantities of data (Dickey, 1991) and mathematical models are frequently used, data assimilation is becoming an important topic. There exist a variety of assimilation techniques including successive correction (Cressman, 1959; Bratseth, 1986), optimal interpolation (Gandin, 1963; Lorenc, 1988a, b), Kalmnan filtering (Kalman, 1960; Kalman and Bucy, 1961; Ghil *et al.*, 1981), and the variational method (Lewis and Derber, 1985; Derber, 1985; Le Dimet and Talagrand, 1986; Lorenc, 1981).

The data assimilation technique used in this study is the variational, or adjoint method. The adjoint method has been used for parameter estimation in a variety of oceanographic systems (Panchang and O'Brien, 1989; Lardner and Das, 1994). More recently, it has been used in simple biological models (Lawson *et al.*, 1995) and coupled physical-biological models (Gunson *et al.*, 1999; Tjipurea *et al.*, 2007; Zhao and Lu, 2008; Li *et al.*, 2012). An adjoint data assimilation method is very useful in determining model inputs (parameters, forcings, *etc.*) that minimizes the misfit between observations and calculations through minimizing a cost function defined as differences between calculated and measured quantities. By finding the optimal solution, the underlying dynamics of the problem can be better understood. The adjoint method consists of the following steps (McGillicuddy *et al.*, 1998; Li *et al.*, 2012): 1) Integrate the forward model to evaluate a cost function using initial estimates of control variables. 2) Run the adjoint equations backwards (derived from the model equation with adjoint operator method or Lagrangian multiplier method, and forced by the misfit between model predictions) to calculate the gradient of the cost function with respect to the control variables. 3) Produce a new estimate of the control variables using a descent algorithm. 4) Repeat the procedure until the convergence to the minimum of the cost function is achieved. This optimization procedure maximizes the agreement between model predictions and observations and provides the optimal estimates of parameters that cannot be observed.

In the Gulf of Maine-Georges Bank region, McGillicuddy *et al.* (1998) utilized an adjoint data assimilation method to determine the mechanisms that control seasonal variations in the abundance of Pseudocalanus spp. It was postulated in the model that the observed distributions result from the interaction of the population dynamics with the climatological circulation. The problem was posed mathematically as a 2-D (x, y) advection-diffusion-reaction equation for biology concentration, with a source or sink term determined through an assimilation approach.

In this paper the linkage between physics and biology and the effect of the horizontal circulation on the biology distribution are studied by applying the model of McGillicuddy *et al.* (1998) to the Gulf of Maine-Georges Bank region. The goal is to investigate and understand how advection and diffusion processes affect the horizontal distribution of phytoplankton with relationship to growth versus mortality region. In the following section, the Chlorophyll-*a* data are obtained from the Marine Resources Monitoring, Assessment, and Prediction program (MARMAP) of the National Oceanographic and Atmospheric Administration, Northeast Fisheries Science Center between 1977 and 1988 (O'Reilly and Zetlin, 1998). The OAX-optimal linear estimation package is used to map and analyze the observations of phytoplankton Chlorophyll-*a* in the Gulf of Maine-Georges Bank region. Section 3 focuses on the adjoint data assimilation approach and the analysis of the model results.

2 Observations of Phytoplankton

2.1 Study Area and Data Sources

The study area includes the Gulf of Maine, Georges Bank, and a small part of the Middle Atlantic Bight north of 39˚N (hereafter referred to as 'North Middle Atlantic Bight'). The Gulf of Maine, Georges Bank, and the Middle Atlantic Bight constitute the three major subdivisions of the Northeast U.S. continental shelf, with different bottom topographies (O'Reilly and Zetlin, 1998). The

Gulf of Maine, a semi-enclosed continental shelf sea, is bounded by the northeast U.S. and Nova Scotia coasts and includes waters west of longitude 66˚W between Georges Bank and the entrance of the Bay of Fundy. The bottom depth throughout much of the Gulf of Maine is greater than 100 m and averages 150 m (Uchupi and Austin, 1987). There are three large basins, the Georges Basin, Wilkinson Basin, Jordan Basin, and several smaller ones in the Gulf of Maine. Shallow water area with a depth of less than 60 m is mostly confined to a relatively narrow band along the coast and over Stellwagen Bank which is to the west of the Jordan Basin and north of Cape Cod. Georges Bank is generally limited by the 200 m isobath except in the west and northwest. From Georges Basin to Georges Bank the water shoals quickly from 200 m to 60 m within a relatively short distance of less than 30 km. The eastern and southern extents are defined by the Northeast Channel and the shelf-break. The Middle Atlantic Bight includes the shelf area between Cape Hatteras and the Great South Channel. The shelf here slopes gently offshore and is shallow compared with the Gulf of Maine and Georges Bank.

The concentration of Chlorophyll-*a*, the dominant photosynthetic pigment in phytoplankton, is widely used by biological oceanographers as a proxy for phytoplankton biomass. The data of Chlorophyll-*a* concentration were collected between 1977 and 1988, most of which were obtained from more than five thousand hydrocast profiles of the upper 100 m of water column. Up to 193 standard sites of the MARMAP surveys are within this study domain (O'Reilly and Zetlin, 1998). The standard locations were defined by the 193 stations and stations 64–193 were used in this study. Tiles (Green and Sibson, 1978) or Dirichlet cells (Ripley, 1981) were constructed around each standard location as shown in O'Reilly and Zetlin (1998). The average distance between each adjacent pair of the 193 tiles is 42 km.

The data refer to the mean Chlorophyll-*a* concentration, abbreviated as Chl_w, over a 2-month period from January–February to November–December, by tile, and by depth for the Gulf of Maine-Georges Bank region. Water column concentration of chlorophyll-*a* (Chl_w) is computed by dividing the water column integral by the depth of integration. In this work Chl_w is the upper 75 m water column mean of the 11 years 1977–1988.

2.2 Distribution of Chl_w

Because the data set is not uniform either in spatial or in temporal coverage, it is necessary to interpolate the irregular data in space and time. The OAX software package by Hannah *et al.* (1995) is used for the optimal linear estimation. Distant space or time observations have little influence on an estimate when compared to those at nearby points and only the best subset of data points with the highest correlation, *i.e.*, the lowest error with the interpolation point, is chosen. The number of the nearest neighbors is critical for obtaining reliable estimation results. Theoretically, the more the nearest neighbors the better the results are. Larger number of the nearest neighbors also leads to longer search time and CPU time because of the inversion of a large covariance matrix. There is not much improvement on the results when the number of the nearest neighbors exceeds a certain value. Hannah *et al.* (1995) suggested that the number of the nearest data points is any number between 10 and 50. The value of 50 is used in this study because using the numbers of nearest neighbors between 50 and 100 does not show significant influence on the distributions of Chl_w.

The estimated distributions of Chl_w are shown in Fig.1 for the six periods of January–February (Jan–Feb),

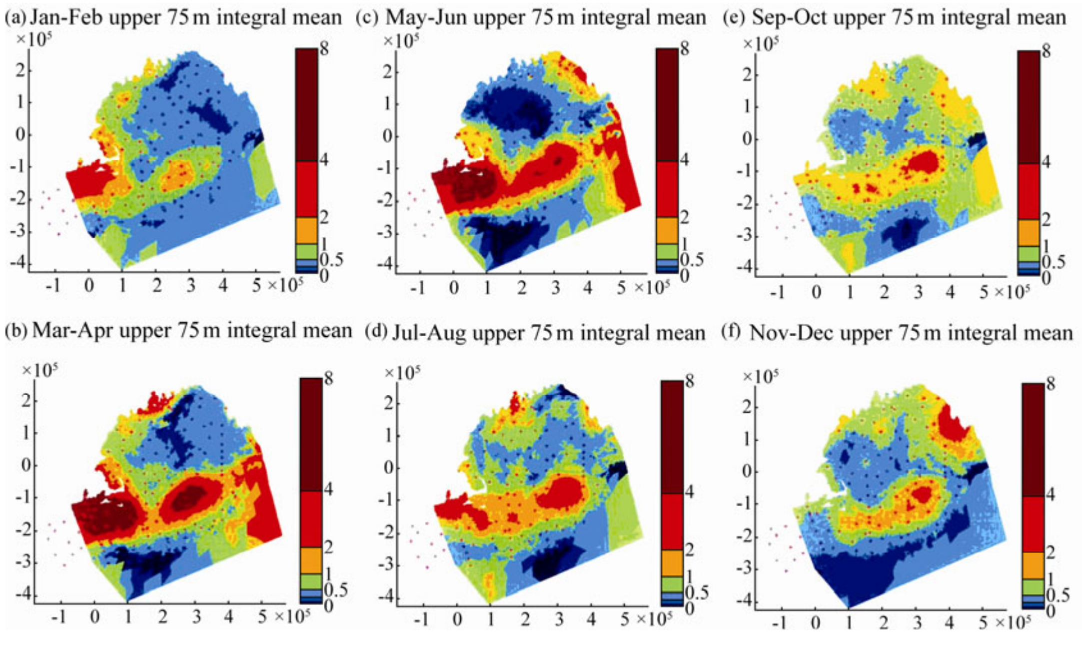

Fig.1 The Chl_w maps of the default case for the periods of a) Jan–Feb, b) Mar–Apr, c) May–Jun, d) Jul–Aug, e) Sep–Oct, and f) Nov–Dec. The unit for both axes is meter.

March–April (Mar–Apr), May–June (May–Jun), July–August (Jul–Aug), September–October (Sep–Oct), and November–December (Nov–Dec), respectively. In order to compare with O'Reilly and Zetlin's (1998) Chlorophyll-*a* maps, the same color bar is used, which is 0, 0.125, 0.25, 0.5, 1, 2, 4, and 8 μg L^{-1}.

2.3 Annual Chl_w Cycle

Because the Northern Outer-shelf is relatively deeper than the Northern Mid-shelf in the North Middle Atlantic Bight, the concentration of Chl_w is generally lower in the Northern Outer-shelf. The highest values of Chl_w during the Jan–Feb period are between 2 and 4 μg L^{-1} in the Northern Mid-shelf. As these values are higher than those observed in the preceding period of Nov–Dec (which are the minimum ones), the higher Chl_w values during the Jan–Feb period are the sign of the winter-spring bloom in the North Middle Atlantic Bight. In Mar–Apr, the Chl_w concentration in the North Middle Atlantic Bight reaches its winter-spring bloom level (4–8 μg L^{-1}). In May-Jun, though in most of the region the bloom level persists, the concentration of Chl_w is generally lower than that of Mar–Apr because the area with the maximum bloom, 4–8 μg L^{-1}, is smaller. The value of Chl_w keeps decreasing after the bloom and the rate of decrease is faster in the southern part of the North Middle Atlantic Bight than in the northern part.

Over Georges Bank, the contours of Chl_w are approximately parallel to the isobaths with higher values in shallower regions, such as the Central Shoals and the Northern Shoals. Since the values of Chl_w over Georges Bank in Jan–Feb are lower than in the preceding Nov–Dec period, the winter-spring bloom has not yet started during the Jan–Feb period. The Winter-Spring bloom starts in March and reaches the maximum in April in most areas except the Great South Channel and the Northeast Peak, where the Winter-Spring bloom starts later and reaches its maximum during the period of May–Jun. The Winter-Spring bloom level is the highest (4–8 μg L^{-1}) in the Central Shoals, the Eastern Outer Shoals, and the Nantucket Shoals. The concentration of Chl_w decreases after the Winter-Spring bloom and the decreasing trend continues until the end of the year in the entire region except the Nantucket Shoals and the Southern Flank. As it decreases after the Winter-Spring bloom, Chl_w decreases faster in southern waters than in northern waters. After the winter-spring bloom in the Nantucket Shoals in April, Chl_w reaches its minimum in Jul–Aug, then increases, and reaches the level for another bloom, the fall bloom, in Sep–Oct. The maximum Chl_w in Sep–Oct is lower than that in April. Although small and insignificant in magnitude there appear two blooms on the Southern Flank, the Winter-Spring bloom in May-Jun and the Fall bloom in Sep–Oct. The Winter-Spring bloom starts in Mar–Apr and becomes signanficant in May–Jun. The Fall bloom occurs in Sep–Oct and has lower *Chlw* concentration than that during the Winter-Spring bloom.

The Gulf of Maine, deeper and located at higher latitudes, has lower values of Chl_w than the North Middle Atlantic Bight and Georges Bank throughout the year. The lowest concentrations of Chl_w, less than 0.5 μg L^{-1}, occur in a large area covering the Georges Basin, Jordan Basin, and Scotian Shelf. The near shore waters of the western Gulf of Maine, especially the isolated area between Cape Cod and the Penobscot Bay, have generally higher phytoplankton concentration (2–4 μg L^{-1}) than the rest of the Gulf of Maine. The Winter-Spring bloom starts here in Jan–Feb. The bloom attains its high level in Mar–Apr with larger Chl_w values between 2 and 4 μg L^{-1}. The area with values lower than 0.5 μg L^{-1} shrinks from the period Jan–Feb to the period Mar–Apr. In May–Jun, the western Gulf of Maine has lower Chl_w concentrations than in Mar–Apr while the northeastern Gulf has higher values. The area with Chl_w values lower than 0.5 μg L^{-1} decreases further in the Gulf in Jul–Aug and reaches its minimum in Sep–Oct.

The Chl_w distributions in Fig.1 compare quite well with those of O'Reilly and Zetlin (1998). Several similarities are listed as examples: a) Chl_w contours are parallel to isobaths; b) The shallower and/or southern regions have relatively higher concentrations than the deeper and/or northern regions; c) The high values of 2–4 μg L^{-1} in Jan–Feb are in the shallow nearshore waters on the northern mid-shelf of the Middle Atlantic Bight and in the isolated region of the western Gulf of Maine between Cape Cod and the Penobscot Bay; d) The Winter-Spring bloom occurs earlier during Jan–Feb in the shallow nearshore waters in the North Middle Atlantic Bight and the isolated region of the western Gulf of Maine between Cape Cod and the Penobscot Bay, and it occurs later in March on Georges Bank. The differences between the distributions of O'Reilly and Zetlin and this study are of minor importance and could be caused by very different mapping approaches. Furthermore, the gridded values are estimated using correlation as the weight in this study while the inverse square distance, (1/*distance*^{2}), was used in O'Reilly and Zetlin's. The most significant difference between these two studies lies in the number of nearest data points used to estimate a gridded value, 50 in this study and 8 in O'Reilly and Zetlin's. More neighbor data points average out small scale variations, and therefore reduce the maximum and increase the minimum.

3 Diagnosis of Physical and Biological Control on Phytoplankton

3.1 The General Circulation in the Studied Region

The circulation field of the Gulf of Maine-Georges Bank region is depicted in Fig.2 (Beardsley *et al.*, 1997; McGillicuddy *et al.*, 1998). A cyclonic circulation pattern is displayed in the Gulf of Maine (Biglow, 1927; Beardsley *et al.*, 1997) and an anti-cyclonic pattern is displayed on Georges Bank. There are two primary and distinct inflows in this region: one is the Scotian Shelf fresh water through the Northern Channel north of

Browns Bank, another is the slope water through the Northeast Channel. Minor sources of inflows are the St. John River, the St. Croix River, the Penobscot River, *etc.* The outflows going to the west mainly follow the 60 m and 100 m isobaths in south of Georges Bank and the Nantucket Shoals. The inflow from the Scotian Shelf continues to pass the mouth of the Bay of Fundy and joins the Maine Coastal Current, together with the input from the St. John River and other river sources. The Maine Coastal Current separates into two branches near the Penobscot Bay. One branch flows seawards and feeds the Jordan Basin cyclonic gyre, and the other branch continues flowing along the coast and separates from it when reaching Cape Cod, with a portion flowing seawards and joining the clockwise circulation on Georges Bank and another portion continuing southwards, joining the outflow along the 60 m isobaths, and turning westward eventually. Before the bifurcation at Cape Cod, a portion of the coastal branch feeds into the circulation of Massachusetts Bay and Cape Cod Bay around the point of Cape Ann. The Great South Channel sill (70 m deep), the Northeast Channel sill (230 m deep), and the Northern Channel (140 m deep) connect the Gulf with the adjacent waters on the continental slope. Exchange of seawater between the Gulf and the North Atlantic is fairly restricted, occurring mostly through the deep Northeast Channel (Ramp *et al.*, 1985; Mountain and Jessen, 1987).

According to McGillicuddy *et al.* (1998), the circulation in the Gulf of Maine-Georges Bank region has been intensively modeled. Using the finite element approach. A typical mesh consists of 16749 elements (McGillicuddy *et al.*, 1998). The fine horizontal resolution around steep topography is 500 m. The model is hydrostatic, fully nonlinear, and utilizes an advanced turbulence closure. The climatological mean circulation is analyzed for six bi-monthly periods and compared with observations (Naimie, 1996; Lynch *et al.*, 1997). The boundary conditions include no flux through solid boundaries, specifications of concentration for inflows, and computations of concentration for outflows assuming no diffusive flux (McGillicuddy *et al.*, 1998). McGillicuddy *et al.* (1998) also proved by control volume experiments that much of the study area is not affected by boundary conditions in a two-month integration.

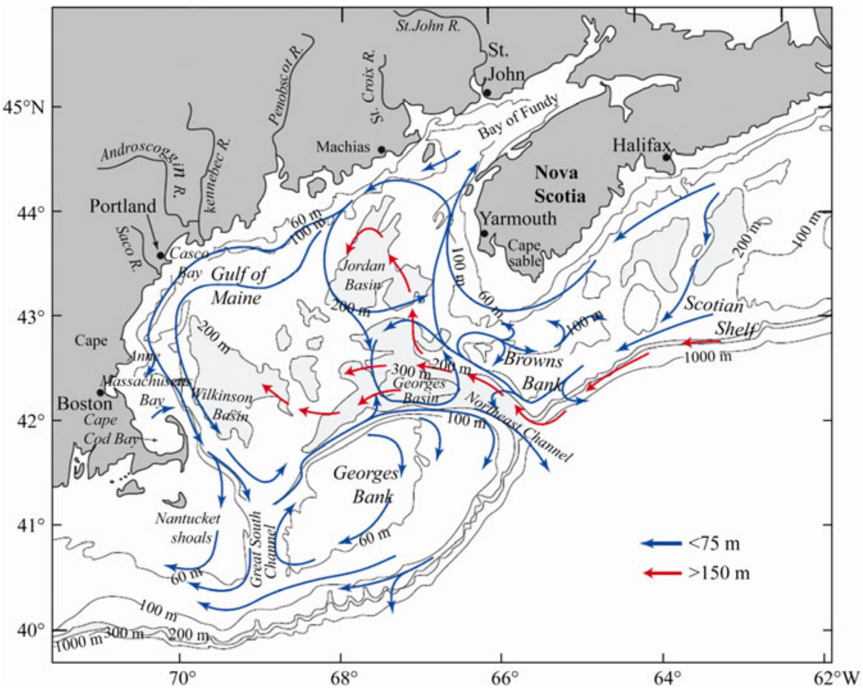

Fig.2 The general circulation in the Gulf of Maine-Georges Bank region during the stratified season from May to September (Beardsley *et al.*, 1997; McGillicuddy *et al.*, 1998).

3.2 An Adjoint Data Assimilation Technique

In the model used for this study (McGillicuddy *et al.*, 1998), the adjoint data assimilation technique is straightforward and reduces the chance of errors in the construction of the adjoint code. The two-dimensional advection-diffusion-reaction (ADR) equation, *i.e.*, the vertically integrated three-dimensional ADR equation, for the positive definite depth-averaged biology concentration $B(x, y, t)$ is expressed as:

$$\frac{\partial B}{\partial t} + \vec{v} \cdot \nabla B - \frac{1}{H} \nabla \cdot (HK \nabla B) = R(x, y) , \tag{1}$$

where $\vec{v}$ is the velocity, K is the diffusivity, and H is the bottom depth. The velocity and diffusivity are calculated using the depth averaged seasonal mean current. The reaction term $R(x, y)$ varies in space only, and serves as a highly idealized parameterization of population dynamics. Positive and negative R implies net growth and net mortality, respectively.

In order to measure the misfit between the predicted concentration B and the observed concentration B_{obs}, a cost function J is defined as:

$$J = \int_{-L_x}^{L_x} \int_{-L_y}^{L_y} \int_{t_0}^{t_1} \delta_M (B - B_{obs})^2 \, dxdydt \,, \quad (2)$$

where L_x and L_y represent the extent of the horizontal domain of interest, and δ_M is a function of space and time, and has the value of one if observations are available, and zero otherwise.

Given initial conditions $B_{obs}(x, y, t_0)$, the forward model calculates the cost function, which gives a measure of the misfit between the calculated concentration B and the measured $B_{obs}(x, y, t_1)$ for the next set of observations at t_1. Integration of the adjoint equation then transforms these measurements of misfit into the gradient of the cost function with respect to the control variable, in this case, R. The gradient is then used to find the direction for the adjustment of R in order to decrease the difference between the model output and the data. However, the cost function is typically not expressed explicitly in terms of R and in order to avoid difficulties in gradient calculations, Lagrange multipliers are introduced with the Lagrange function, L, defined as:

$$L = J + \int_{-L_x}^{L_x} \int_{-L_y}^{L_y} \int_{t_0}^{t_1} \lambda (\frac{\partial B}{\partial t} + \vec{v}.\nabla B - \frac{1}{H} \nabla \cdot (HK\nabla B) - R) dxdydt \,, \quad (3)$$

where $\lambda = \lambda(x, y, t)$ is the unknown Lagrange multiplier.

The model equations, the adjoint equations, and the gradient of the cost function are obtained by finding a saddle point of the Lagrange function, that is, a point in B, R, λ space where the partial derivatives of L vanish simultaneously, *i.e.*, $\partial L/\partial B = \partial L/\partial R = \partial L/\partial \lambda = 0$. The term R that minimizes L at the saddle point is also obtained. The requirement of $\partial L/\partial \lambda = 0$ returns the adjoint model, which is an advection-diffusion reaction equation for the Lagrange multiplier forced by the misfit between the calculated and observed values of B with homogeneous boundary conditions:

$$-\frac{\partial \lambda}{\partial t} - \nabla.\lambda \vec{v} - \frac{1}{H} \nabla.(HK\nabla \lambda) = -2\delta_M (B - B_{obs}) \,. \quad (4)$$

The gradient of the cost function with respect to the control variable R can also be derived through the integration of the adjoint model

$$\frac{\partial J}{\partial R} = \int_{t_0}^{t_1} \lambda(x, y, t) dt \,. \quad (5)$$

Once the direction for the R adjustment is found, the step size, the size of change in that particular direction, must be determined. After the variables are adjusted by the calculated step size and direction, the model is again applied and the process repeated. Hence, by repeating the iterative procedure, including a model run, an adjoint run and a step size calculation, convergence is reached for the values of $R(x, y)$ that minimize the cost function. This also provides the best fit of B to the observed B_{obs} under the constraint that the forward model equation is satisfied. The optimal step size is determined using the steepest descent method as in Derber (1985).

3.3 Results

The inversion work is separated into six bi-monthly periods. In each assimilation experiment, initial conditions are specified, and $R(x, y)$ is sought in order for the forward model integration to fit the data of the next period. For example, from the period of Jan–Feb to Mar–Apr, the initial condition is from the Jan–Feb observations, and $R(x, y)$ is obtained to fit the Mar–Apr observations. The interpretation of the effect of circulation on passively drifting biomass is confined to the region not affected by boundary effects because the distribution of phytoplankton is not very well sampled in some of the inflow regions. The inversion results, after the cost function values are reduced by approximately an order of magnitude, are illustrated in six figures, Figs.3–8, with each figure representing each of the six periods, Jan–Feb to Mar–Apr, Mar–Apr to May–Jun, May–Jun to Jul–Aug, Jul–Aug to Sep–Oct, Sep–Oct to Nov–Dec, and Nov–Dec to Jan–Feb, respectively. Shown from these results are the distributions of the source term, the advective flux divergence term, the diffusive flux divergence term, and the tendency term in the advection-diffusion-reaction equation. The tendency term is calculated as the sum of the other three terms.

3.3.1 Jan–Feb to Mar–Apr

The source term map (Fig.3c) shows strong growth (red shading) on the crest of Georges Bank, moderate growth (yellow shading) in the coastal area of Massachusetts Bay, and weak growth (green shading) in most of the Gulf of Maine, especially in the western Gulf. On Georges Bank, a balance exists between the advection and the source term. Flow onto the crest across the northern flank of the Bank brings in phytoplankton of low concentrations from the Gulf of Maine. The positive advective flux divergence on the southern part of the Bank transports high concentration water from the crest towards the Great South Channel on the southwest (McGillicuddy *et al.*, 1998). However, the net growth and net mortality coincide with the negative and positive advective flux divergence, respectively. The net growth has larger magnitude than that corresponding to the negative advective flux divergence and the net mortality has smaller magnitude than that corresponding to the positive advective flux divergence; therefore, the overall tendency on Georges Bank is the concentration increasing from Jan–Feb to Mar–Apr. In the coastal region of Massachusetts Bay, the negative contribution from advection is weaker than that corresponding to the net moderate growth. The tendency is then largely controlled by the net moderate growth. The concentration in this region increases slightly during this period. In the Gulf of Maine, the tendency of phytoplankton growth varies with space. Only some regions in the interior of the Gulf and off the western coast have positive tendencies.

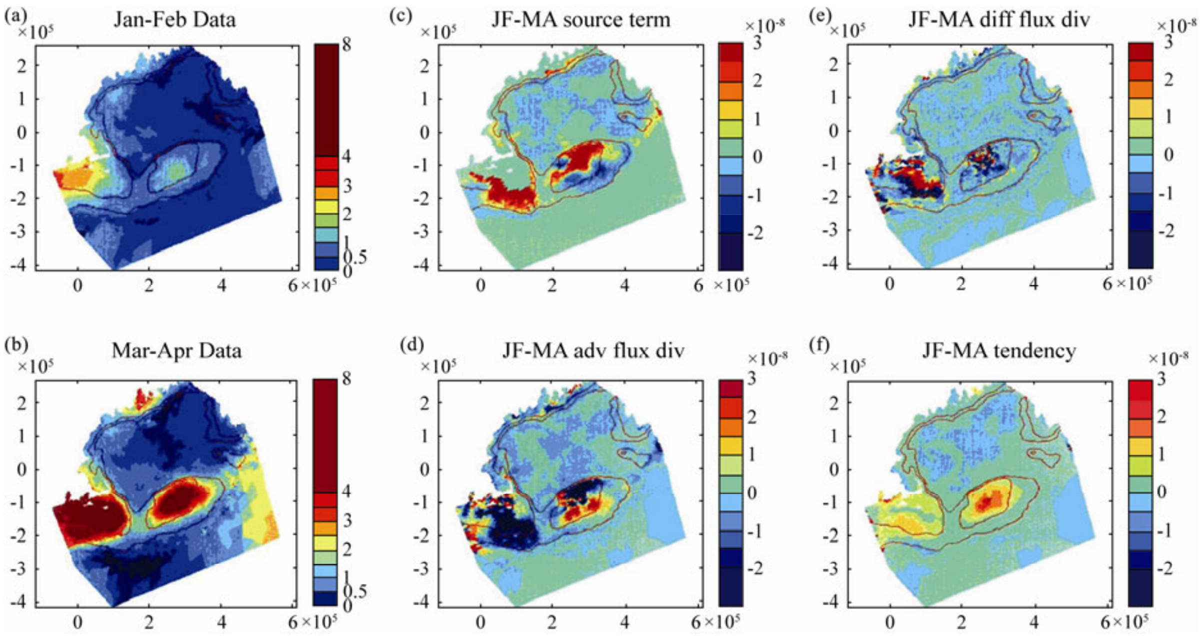

Fig.3 The left two panels show the observed data for periods of a) Jan–Feb and b) Mar–Apr. The other four panels are the inversion results for the period from Jan–Feb to Mar–Apr, representing c) the source term, d) the advective flux divergence, e) the diffusive flux divergence, and f) the tendency, respectively. The unit for both axes is meter.

3.3.2 Mar–Apr to May–Jun

In the coastal region of Cape Ann and Massachusetts Bay, the positive source term has greater magnitude than in the previous period. However, the strong negative divergence of advective flux brings in low-concentration water here from the interior of the Gulf of Maine. The net tendency for this region is that the concentration decreases from Mar–Apr to May–Jun, with the negative contribution from the advective flux divergence overshadowing the growth. Comparing with the previous period, the source term decreases on Georges Bank with smaller positive values at the center and in the northern part of the Bank. Due to the increasing stratification from the previous period, the clockwise flow pattern on the Bank is more retentive. The position of the dipole structure of the advective flux divergence (red and blue) on the Bank rotates slightly clockwise and the negative contribution from the Gulf of Maine decreases in magnitude. The combined influence on Georges Bank is that the concentration decreases over most of the region, except for a small area of the western Bank where the concentration has a small increase. In the Gulf of Maine, the tendency is negative and relatively unnoticeable (Fig.4).

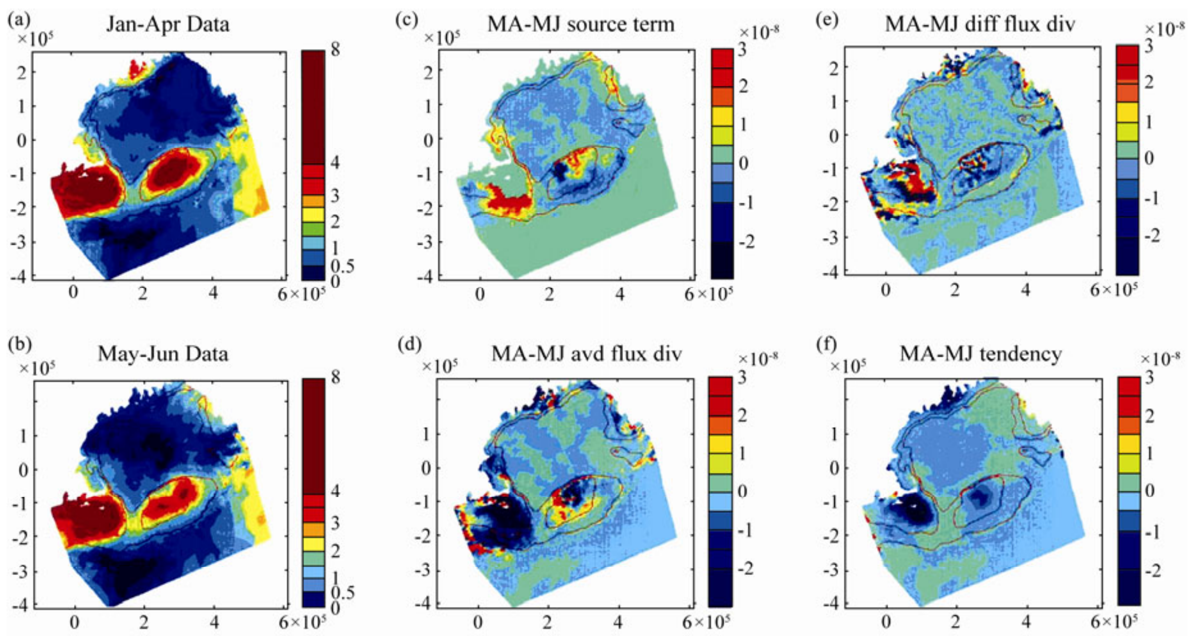

Fig.4 The left two panels show the observed data for periods of a) Mar-Apr and b) May-Jun. The other four panels are the inversion results for the period from Mar-Apr to May-Jun, representing respectively c) the source term, d) the advective flux divergence, e) the diffusive flux divergence, and f) the tendency. The unit for both axes is meter.

3.3.3 May–Jun to Jul–Aug

In the coastal region of Cape Ann, Massachusetts Bay, and Cape Cod Bay, the magnitude of net growth is smaller than that from Mar–Apr to May–Jun. Because flow still brings low concentration phytoplankton from the Gulf of Maine into this region, which overweighs the weak growth, the overall tendency of this region is negative and has a magnitude close to that in the previous period. On Georges Bank, the dipole structure of the advective flux divergence further rotates clockwise and the magnitude is smaller than that in the preceding period. The source term has a negative contribution except in a small region on the northeastern edge of the Bank. With the small area of net growth overshadowed by the negative advective flux divergence from the Gulf and the net mortality exceeding that corresponding to the positive advective flux divergence from the crest to the Great South Channel, the concentration in the entire Georges Bank has a decreasing tendency. Except in the coastal region of Cape Ann, Massachusetts Bay, and Cape Cod Bay, the tendency in the Gulf of Maine is for the concentration to increase slightly (Fig.5).

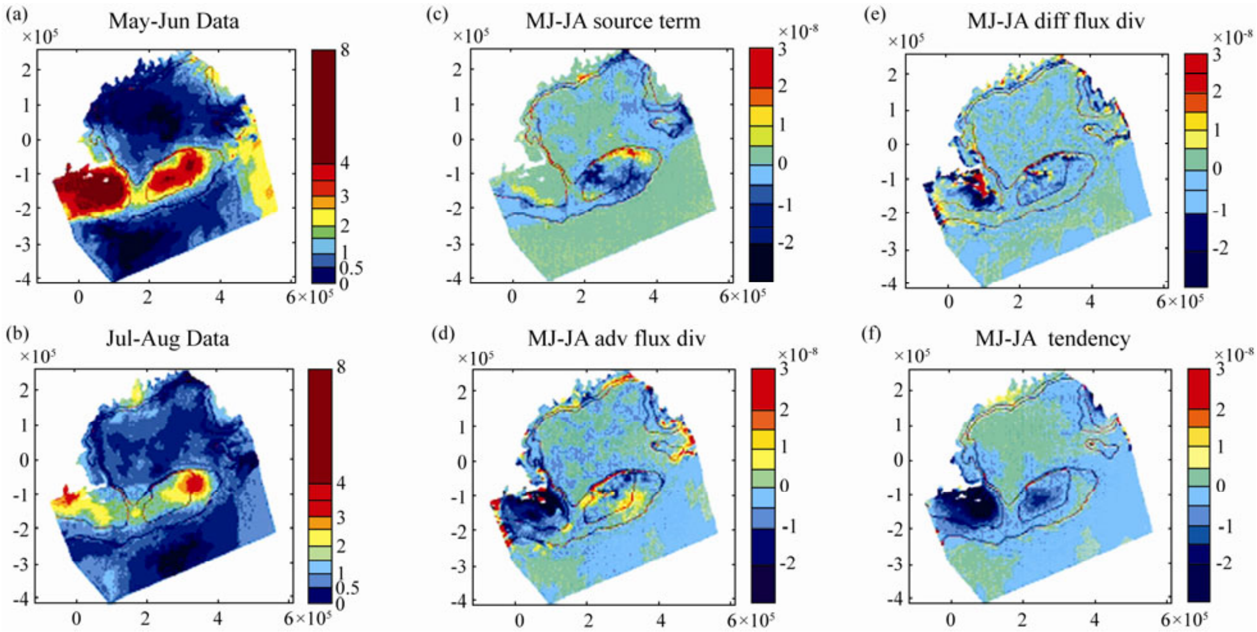

Fig.5 The left two panels show the observed data for periods of a) May–Jun and b) July–Aug. The other four panels are inversion results for the period from May–Jun to Jul–Aug, representing respectively c) the source term, d) the advective flux divergence, e) the diffusive flux divergence, and f) the tendency. The unit for both axes is meter.

3.3.4 Jul–Aug to Sep–Oct

On Georges Bank, the source term and the advective flux divergence term almost exactly mirror each other. On the southern and northern Bank, the source term is positive and the advection term is negative. On the eastern and western Bank, the source term is negative and the advection term is positive. Except in a small area on the northern and southern edge, the tendency is to decrease with the net mortality overcoming the effect of positive advection and the net growth overcome by the effect of negative advection. There is a small area with a very weak increase in concentration on the northern and southern edge. In the Gulf of Maine, the concentration distribution in the western coast does not change much from the previous period. Inside the Gulf of Maine the tendency of increase from May–Jun to Jul–Aug is changed to a partially increasing and partially decreasing trend, with the western part having a greater decreasing tendency and the eastern part having a greater increasing tendency. Both the increase and decrease are very weak (Fig.6).

3.3.5 Sep–Oct to Nov–Dec

The source term infers moderate growth on the northern and northeastern Georges Bank and net mortality on the rest of the Bank. Although the strong summer stratification on Georges Bank is able to resist the influence from the Gulf of Maine, the contribution of the negative advective flux divergence to the growth on the Bank still persists on the north flank. The dipole structure of the advective flux divergence on the Bank does not rotate clockwise as much as in the preceding period, which suggests that the circulation on the Bank is not as retentive. On the northern Bank, the net growth is overshadowed by the low concentration inflow from the Gulf of Maine or from the western part of the Bank and the concentration has a decreasing tendency. On the southern Bank, the positive concentration input from the Bank crest counteracts the mortality in the region and the growth tendency slightly dominates. In the rest of the area on the Bank, the net mortality has a larger magnitude than that corresponding to the positive advective flux divergence, and the concentration tends to decrease.

In the coastal regions of Massachusetts Bay and Cape Cod Bay, because of the impact of the low concentration inflow from the Gulf of Maine at Cape Ann and the weak mortality, decreasing of concentration is the overall trend. In the Gulf of Maine, the tendency varies in space, but during this period the decrease in concentration is the leading trend (Fig.7).

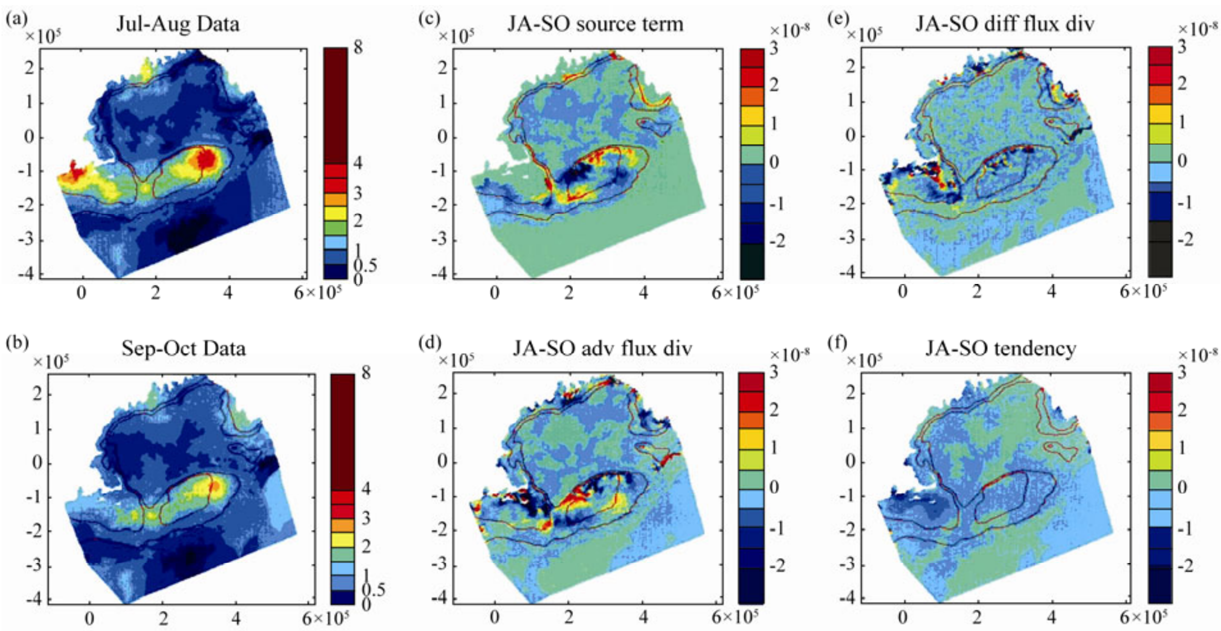

Fig.6 The left two panels show the observed data for periods of a) Jul-Aug and b) Sep-Oct. The other four panels are the inversion results for the period from Jul-Aug to Sep-Oct, representing respectively c) the source term, d) the advective flux divergence, e) the diffusive flux divergence, and f) the tendency. The unit for both axes is meter.

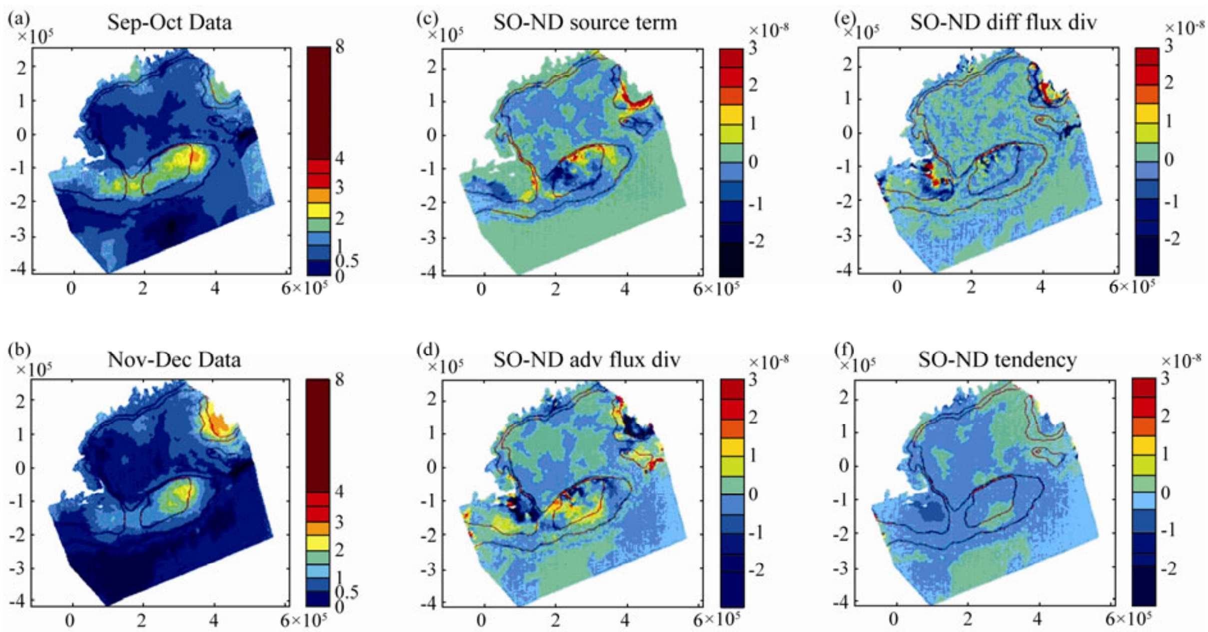

Fig.7 The left two panels show the observed data for periods of a) Sep-Oct and b) Nov-Dec. The other four panels are the inversion results for the period from Sep-Oct to Nov-Dec, representing respectively c) the source term, d) the advective flux divergence, e) the diffusive flux divergence, and f) the tendency. The unit for both axes is meter.

3.3.6 Nov–Dec to Jan–Feb

In this period, the growth in the coastal area of Cape Ann is comparable to that in the period from Jan–Feb to Mar–Apr and is the second strongest in all the six periods, secondary to that from Mar–Apr to May–Jun. The growth on Georges Bank is weaker than that in the coastal region of Cape Ann. The inflow at Cape Ann brings in low-concentration water from the interior of the Gulf of Maine. The combined effect of the growth and the inflows increases the concentration in this coastal region, so as to accelerate the arrival of the spring bloom. On Georges Bank, with the declining seasonal stratification, the circulation is less retentive than in the summer season. The negative advective flux divergence across the north flank overshadows the net growth. The positive advective flux divergence from the Bank crest to the Great South Channel has a smaller magnitude than that corresponding to the net mortality in most of the places where they overlay each other. Therefore, the concentration on Georges Bank decreases except over a limited area in the southwest, which is on the pathway of the outflow from the crest to the southwest. On the northeastern Bank, the decreasing trend reaches its peak in a small region, *i.e.*, the negative tendency has its maximum magnitude. The concentration increases in the western Gulf of Maine and decreases in the eastern Gulf of Maine (Fig.8).

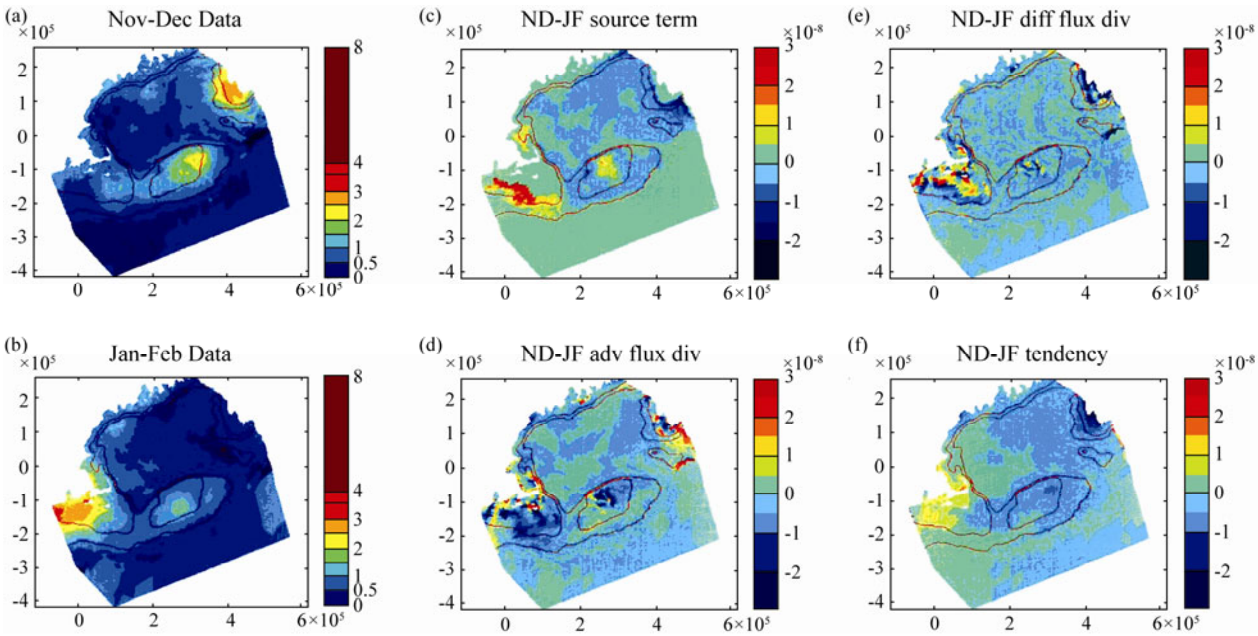

Fig.8 The top two panels show the observed data for periods of a) Nov-Dec and b) Jan-Feb. The lower four panels are the inversion results for the period from Nov-Dec to Jan-Feb, representing respectively c) the source term, d) the advective flux divergence, e) the diffusive flux divergence, and f) the tendency. The unit for both axes is meter.

The calculated concentrations by the forward model are very close to the corresponding observations for the six simulation periods. As an example only results from the first period, which is initialized with the Jan–Feb observations, are shown in Fig.9 to compare with the Mar–Apr data (Fig.3b). The cost function values are reduced by approximately an order of magnitude after 50 iterations with the exception of the periods from Jul–Aug to Sep–Oct and from Sep–Oct to Nov–Dec (Fig.10). In these last two periods, the cost function values are reduced by the same amount after 200 iterations.

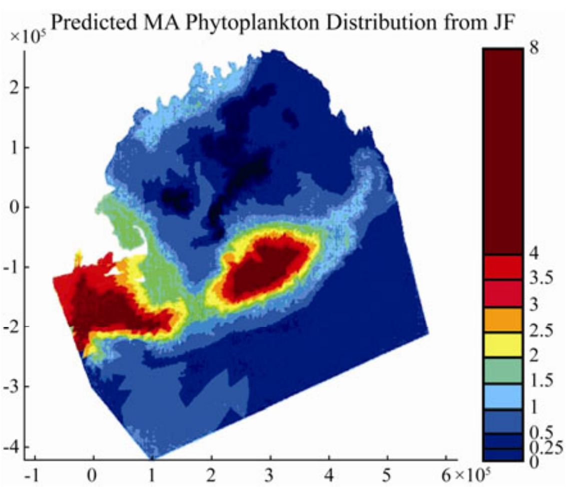

Fig.9 The predicted phytoplankton distribution for the period of Mar-Apr. The unit for both axes is meter.

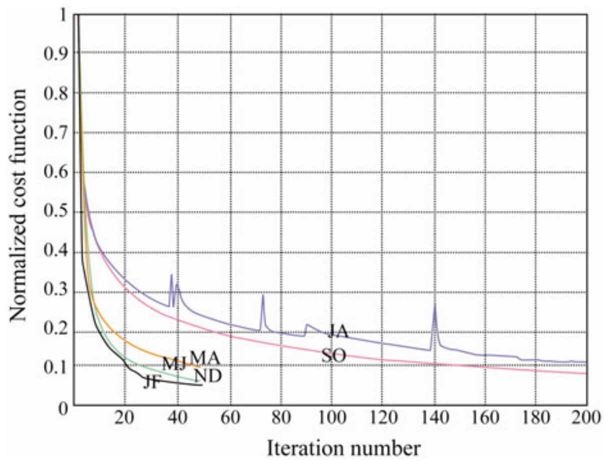

Fig.10 The cost functions for each of the six assimilation experiments (normalized by the initial value in each case).

4 Discussion and Conclusions

In this paper, the interaction between physical and biological processes is studied for the Gulf of Maine-

Georges Bank region and the effect of the circulation on the distribution of phytoplankton is explored.

The research reveals that the seasonal and geographic variations of phytoplankton concentration in the Gulf of Maine-Georges Bank region are consistent with the MARMAP data. Two population centers are found in the study area: one is on Georges Bank and the other is in the western coastal region of the Gulf of Maine, *i.e.*, the coastal regions of Cape Ann, Massachusetts Bay, and Cape Cod Bay. During the period of Jan–Feb to Mar–Apr, the growth is shown for both Georges Bank and the western coastal region of the Gulf of Maine with the stronger growth on Georges Bank. Therefore, this period is defined as a time of strong growth on Georges Bank and of moderate growth in the western coastal region of the Gulf of Maine. After the spring bloom peaks in Mar–Apr, comes the time of decline from Mar–Apr to Nov–Dec. From Mar–Apr to Jul–Aug, there is a period of faster decline, while the concentration decreases slightly from Jul–Aug until the end of the year, which is a relatively stable period. The changing trend from Nov–Dec to Jan–Feb on Georges Bank is opposite to that in the coastal region of the western Gulf of Maine with a decrease of the phytoplankton abundance on Georges Bank but a increase in the coastal region of the western Gulf of Maine. The decline on Georges Bank is even stronger than that during the period from Jul–Aug to Nov–Dec.

It is found that the seasonal cycle of the phytoplankton distribution is controlled by both biological sources and ocean current, and their relative significance varies with space and time. On Georges Bank, the area of net growth (negative advective flux divergence) always lies north of the area of net mortality (positive advective flux divergence) and the net growth (net mortality) mirrors the negative (positive) advective flux divergence in space. The net growth and the net mortality thus counter-balance the negative and positive advection, respectively, throughout the year despite the seasonal or spatial variability.

As shown in Wang and Malanotte-Rizzoli (1999), the phytoplankton growth or mortality is very closely related to the availability of nutrients and sunlight in the mixed layer. During winter, strong mixing continuously brings nutrients into the euphotic layer from below, while in summer, the stratification inhibits the nutrient flux and limits the nutrient supply from below. Therefore, on Georges Bank, most of the biological growth occurs between January and April when there are sufficient nutrients and light, while in the other months the weak growth or net mortality dominates due to the lack of nutrients and/or light. In the coastal region of the western Gulf of Maine, the source term is positive throughout the year except the period from Sep–Oct to Nov–Dec, which could be related to the availability of both nutrients and light and the consequent complete vertical mixing in this shallow region.

The value of advective flux divergence is also a function of vertical mixing or stratification, especially on Georges Bank. During winter the deep mixing results in the less retentive circulation pattern on Georges Bank, and hence the phytoplankton distribution on the Bank is more susceptible to the influence of the flow from the Gulf of Maine than during summer with stratification. The advective flux divergence term, due to both the advection from the Gulf of Maine on the northern flank and the advection from the crest to the southwest, has the largest magnitude in the period from Jan–Feb to Mar–Apr. Its magnitude decreases with the arrival of summer. Generally speaking, the magnitude of the negative advective flux divergence from the Gulf of Maine is larger on the northern flank of Georges Bank than in the coastal region of the western Gulf of Maine. However, it is important to note that advection constitutes the controlling factor for tendency more frequently in the coastal region of the western Gulf than on the Bank, because of the small magnitude of the source term in the former region.

In the coastal region of the western Gulf of Maine, the tendency is generally controlled by the negative advective flux divergence, with the exception that from Nov–Dec to Mar–Apr, the contribution from advection is overshadowed by the moderately high net growth. The case with Georges Bank is quite different. The only time when the negative influence by the advection from the Gulf of Maine plays a controlling role together with the net mortality, corresponds to the period of decline from Mar–Apr to May–Jun. During the period of increase from Jan–Feb to Mar–Apr, the advection from the Gulf of Maine is overshadowed by the positive source term. It is the net growth and the positive advection together that cause the increase of the phytoplankton concentration. From May–Jun to Jan–Feb, the decline trend is determined by the net mortality and also by the negative contribution from the Gulf of Maine. In this period, while the low concentration from the Gulf of Maine does help to overcome the net growth on the northern flank, the major factor is the net mortality that overbalances the advection from the crest.

Diffusion does not have a systematic impact on biomass distribution, because the diffusive flux divergence term generally has a smaller magnitude than the source term and the advective flux divergence term. Sometimes it does have comparable magnitudes, such as in the period from Jan–Feb to Mar–Apr on Georges Bank, but it is rather noisy and organized in small patches that do not affect the main features of the biomass distribution. The only possible effect of diffusion is to smooth out biomass concentration. This research suggests that the two separated biomass populations in the coastal area of the western Gulf of Maine and on Georges Bank are self-sustaining, and that Gulf of Maine is not the source for them.

Acknowledgements

We thank Dr. Dennis McGillicuddy at the Woods Hole Oceanographic Institution (USA) and Professor Xianqing Lv at Ocean University of China for helpful discussions. This work was supported by the Shangdong

Province Young and Middle-Aged Scientists Research Awards under Grant BS2011HZ021.

References

Beardsley, R. C., Butman, B., Geyer, W. R., and Smith, P., 1997. Physical oceanography of the Gulf of Maine: An update. In: *Proceeding of the Gulf of Maine Ecosystem Dynamics Scientific Symposium and Workshop*. Braasch, G., and Wallace, G., eds., Regional Association for Research in the Gulf of Maine, Hanover NH, RARGOM Report 97-1.

Bengtsson, L., Ghil, M., and Källen, E., 1981. *Dynamic Meteorology: Data Assimilation Methods*. Springer, New York, 330pp.

Biglow, H. B., 1927. Physical oceanography of the Gulf of Maine. *Bulletin of the United States Bureau of Fisheries*, **40**: 511-1027.

Bratseth, A. M., 1986. Statistical interpolation by means of successive corrections. *Tellus*, **38**A: 439-447.

Campbell, D. E., 1986. Process variability in the Gulf of Maine–a macroesturiane environment. *Esturian Variability*, 261-275.

Cohen, E. B., and Grosslein, M. D., 1987. Production on Georges Bank compared with other shelf ecosystems. In: *Georges Bank*. Backus, R. H., ed., MIT Press, Cambridge, MA, 383-391.

Cohen, E. B., Grosslein, M. D., Sissenwine, M. P., Steimle, F., and Wright, W. R., 1982. Energy budget of Georges Bank. *Canadian Special Publication of Fisheries and Aquatic Sciences*, **59**: 95-107.

Collins, A. K., Allen, S. E., and Pawlowicz, R., 2009. The role of wind in determining the timing of the spring bloom in the Strait of Georgia. *Canadian Journal of Fisheries and Aquatic Sciences*, **66** (9): 1597-1616.

Cressman, G. P., 1959. An operational objective analysis system. *Monthly Weather Review*, **87**: 367-374.

Denman, K. L., and Pena, M. A., 2002. The response of two coupled one-dimensional mixed layer/planktonic ecosystem models to climate change in the NE subarctic Pacific Ocean. *Deep Sea Research-II*, **49** (24-25): 5739-5757, DOI: 10.1016/S0967-0645(02)00212-6.

Derber, J. C., 1985. The variational four-dimensional assimilation of analyses using filtered models as constraints. PhD thesis, University of Wisconsin, Madison, Wisconsin.

Dickey, T. D., 1991. The emergence of concurrenct high-resolution physical and bio-optical measurements in the upper ocean and their applications. *Reviews of Geophysics*, **29**: 383-413.

Flierl, G. R., and Davis, C. S., 1993. Biological effects of Gulf Stream meandering. *Journal of Marine Research*, **51**: 529-560.

Franks, P., and Chen, C., 1996. Plankton production in tidal fronts: A model of Georges Bank in summer. *Journal of Marine Research*, **54** (4): 631-651.

Gandin, L. S., 1963. *Objective Analysis of Meteorlogical Fields*. Translated from the Russian. Israel program for Scientific Translations, Jerusalem, 1965, 242pp.

Ghil, M., and Malanotte-Rizzoli, P., 1991. Data assimilation in meteorology and oceanography. *Advances in Geophysics*, **33**: 141-266.

Ghil, P. E., Murray, W., and Wright, M. H., 1981. *Practical Optimization*. Academic Press, Orlando.

Green, P. J., and Sibson, R., 1978. Computing Dirichlet tessellations in the plane. *Computer Journal*, **21**: 168-173.

Gunson, J., Oschlies, A., and Garon, V., 1999. Sensitivity of ecosystem parameters to simulated satellite ocean color data using a couple physical-biological model of the North Atlantic. *Journal of Marine Research*, **57**: 613-39.

Haidvogel, D. B., and Robinson, A. R., 1989. Special issue: Data assimilation. *Dynamics of Atmospheres and Oceans*, **13**: 171-513.

Hannah, C., Graca, M., and Loder, J., 1995. The OAX software package. Fisheries and Oceans Canada, Ocean and Ecosystem Sciences.

Home, E. P. W., Loder, J. W., Harrison, W. G., Mohn, R., Lewis, M. R., Irwin, B., and Platt, T., 1989. Nitrate supply and demand at the Georges Bank tidal front. *Scientia Marina*, **53** (2-3): 145-158.

Kalman, R. E., 1960. A new approach to linear filtering and prediction problems. *Journal of Basic Engineering-Transactions of the ASME*, *Series D*, **82**: 35-45.

Kalman, R. E., and Bucy, R. S., 1961. New results in linear filtering and prediction theory. *Journal of Basic Engineering-Transactions of the ASME*, *Series D*, **83**: 95-108.

Lardner, R. W., and Das, S. K., 1994. Optimal estimation of eddy viscosity for a quasi-three-dimensional numerical tidal and storm surge model. *International Journal for Numerical Methods in Fluids*, **18**: 295-312.

Lawson, L. M., Spitz, Y. H., Hofmann, E. E., and Long, R. B., 1995. A data assimilation technique applied to a predator-prey model. *Bulletin of Mathematical Biology*, **57**: 593-617.

Le Dimet, F. X., and Talagrand, O., 1986. Variational algorithms for analysis and assimilation of meteorological observations: Theoretical aspects. *Tellus A*, **37**: 309-322.

Lewis, J. M., and Derber, J. C., 1985. The use of adjoint equations to solve a variational adjustment problem with adjective constraints. *Tellus A*, **37**: 309-322.

Li, X. Y., Wang, C. H., and Lv, X. Q., 2012. Inversion of the spatially varying parameters in a marine ecosystem model. *Procedia Environmental Sciences*, **13**: 2062-2076

Lorenc, A. C., 1981. A global three-dimensional multivariate statistical interpolation scheme. *Monthly Weather Review*, **109**: 701-721.

Lorenc, A. C., 1986. Analysis methods for numerical weather prediction. *Quarterly Journal of the Royal Meteorological Society*, **112**: 1177-1194.

Lorenc, A. C., 1988a. Optimal non-linear objective analysis. *Quarterly Journal of the Royal Meteorological Society*, **114**: 205-240.

Lorenc, A. C., 1988b. A practical approximation to optimal 4-dimemsional objective analysis. *Monthly Weather Review*, **116**: 730-745.

Lynch, D. R., Holboke, M. J., and Naimie, C. E., 1997. The Maine coastal current: Spring climatological circulation. *Continental Shelf Research*, **18**: 607-639.

Lynch, D. R., Ip, J. T. C., Naimie, C. E., and Werner, F. E., 1996. Comprehensive coastal circulation model with application to the Gulf of Maine. *Continental Shelf Research*, **16**: 875-906.

Mann, K. H., and Lazier, J. R. N., 1991. *Dynamics of Marine Ecosystem Biological-Physical Interaction in the Oceans*. Blackwell Scientific Publications, 466pp.

Margalef, R., 1967. Laboratory analogues of estuarine plankton systems. In: *Esturies*. Lauff, G. H., ed., American Association for the Advancement Science Publication, Washington, D. C., No. 83, 515-521.

McClain, C. R., Esaias, W. E., Feldman, G. C., Elrod, J., Endres, D., Firestone, J., Darzi, M., Evans, R., and Brown, J., 1990. Physical and biological processes in the North Atlantic during the first GARP global experiment. *Journal of Geo-*

physical Research, **95**: 18027-18048.

McGillicuddy, D. J., Lynch, D. R., Moore, A. M., Gentleman, W. C., Davis, C. S., and Meise, C. J., 1998. An adjoint data assimilation approach to diagnosis of physical and biological controls on *Pseudocalanus* spp. in the Gulf of Maine-Georges Bank region. *Fisheries Oceanography*, **7** (3/4): 205-218.

Mellor, G. L., and Yamada, T., 1982. Development of a turbulence closure model for geophysical fluid problems. *Reviews of Geophysics*, **20**: 851-875.

Menzel, D. W., and Ryther, J. H., 1960. The annual cycle of primary production in the Sargasso Sea off Bermuda. *Deep-Sea Research*, **6**: 351-367.

Mitchell, B. C., Brody, E. A., Holm-Hansen, O., McClain, C., and Bishop, J., 1991. Light limitation of phytoplankton biomass and macronutrient utilization. *Limnology and Oceanography*, **36**: 1662-1677.

Mountain, D. G., and Jessen, P. F., 1987. Bottom waters of the Gulf of Maine, 1978–1983. *Journal of Marine Research*, **45**: 319-345.

Naimie, C. E., 1996. Georges Bank residual circulation during weak and strong stratification periods: Prognostic numerical model results. *Journal of Geophysical Research*, **101**: 6469-6486.

O'Reilly, J. E., and Zetlin, C., 1998. Seasonal, horizontal, and vertical distribution of phytoplankton chlorophyll *a* in the northeast U.S. continental shelf ecosystem. NOAA Technical Report, NMFS 139, 126pp.

O'Reilly, J. E., Zetlin, C., and Busch, D. A., 1987. Primary production. In: *Georges Bank*. Backus, R. H., ed., MIT Press, Cambridge, MA, 220-233.

Panchang, V. G., and O'Brien, J. J., 1989. On the determination of hydraulic model parameters using the adjoint state formulation. In: *Modeling Marine Systems*. Davis, A. M., ed., CRC Press, Boca Raton, Florida, 6-18.

Ramp, S. R., Schlitz, R. J., and Wright, W. R., 1985. The deep flow through Northeast Channel, Gulf of Maine. *Journal of Physical Oceanography*, **15**: 1790-1808.

Riley, G. A., 1941. Plankton studies – IV. Georges Bank. *Bulletin of the Bingham Oceanographic Collection*, **7**: 1-73.

Riley, G. A., 1967. Mathematical model of nutrient conditions in coastal waters. *Bulletin of the Bingham Oceanographic Collection*, **19**: 72-80.

Ripley, B. D., 1981. *Spatial Statistics*. John Wiley and Sons, New York, 252pp.

Tjipurea, J. F., Polzin, D., and Winguth, A. M. E., 2007. Assimilation of seasonal chlorophyll and nutrient data into an adjiont three-dimension ocean carbon cycle model: Sensitivity analysis and ecosystem parameter optimization. *Global Biogeochemical Cycles*, **21**: GB1001.

Uchupi, E., and Austin, J. A., 1987. Morphology. In: *Georges Banks*. Backus, R. H., and Bourne, D. W., eds., MIT Press, Cambridge, MA, 25-30.

Wang, C., and Malanotte-Rizzoli, P., 1999. Diagnosis of physical and biological controls on phytoplankton distribution in the Gulf of Maine-Georges Bank region. Master thesis, MIT/WHOI Joint Program.

Zhao, Q., and Lu, X. Q., 2008. Parameter estimation in a three-dimensional marine ecosystem model using the adjoint technique. *Journal of Marine Systems*, **74** (1-2): 443-452, DOI: 10.1016/j.jmarsys.2008.03.006.

(Edited by Xie Jun)